JACS
JOURNAL OF THE AMERICAN CHEMICAL SOCIETY
Communication
pubs.acs.org/JACS

Molecular Engineering of a TBET-Based Two-Photon Fluorescent Probe for Ratiometric Imaging of Living Cells and Tissues

Liyi Zhou, Xiaobing Zhang, Qianqian Wang, Yifan Lv, Guojiang Mao, Aili Luo, Yongxiang Wu, Yuan Wu, Jing Zhang, and Weihong Tan*

Molecular Sciences and Biomedicine Laboratory, State Key Laboratory for Chemo/Biosensing and Chemometrics, College of Chemistry and Chemical Engineering, College of Biology, Collaborative Innovation Center for Molecular Engineering and Theranostics, Hunan University, Changsha, Hunan 410082, China

Supporting Information

ABSTRACT: In contrast to one-photon microscopy, two-photon probe-based fluorescent imaging can provide improved three-dimensional spatial localization and increased imaging depth. Consequently, it has become one of the most attractive techniques for studying biological events in living cells and tissues. However, the quantitation of these probes is primarily based on single-emission intensity change, which tends to be affected by a variety of environmental factors. Ratiometric probes, on the other hand, can eliminate these interferences by the built-in correction of the dual emission bands, resulting in a more favorable system for imaging living cells and tissues. Herein, for the first time, we adopted a through-bond energy transfer (TBET) strategy to design and synthesize a small molecular ratiometric two-photon fluorescent probe for imaging living cells and tissues in real time. Specifically, a two-photon fluorophore (D-π-A-structured naphthalene derivative) and a rhodamine B fluorophore are directly connected by electronically conjugated bond to form a TBET probe, or **Np-Rh**, which shows a target-modulated ratiometric two-photon fluorescence response with highly efficient energy transfer (93.7%) and two well-resolved emission peaks separated by 100 nm. This novel probe was then applied for two-photon imaging of living cells and tissues and showed high ratiometric imaging resolution and deep-tissue imaging depth of 180 μm, thus demonstrating its practical application in biological systems.

Organic small-molecule fluorescent probe-based imaging is a widely used technology to study biological events with high spatiotemporal resolution. However, most traditional fluorescent probes have been single-photon-excited at short wavelengths, which resulted in photobleaching, interference from autofluorescence in cells and tissues, and shallow penetration depth (<100 μm). A much more feasible alternative would utilize two-photon probe-based fluorescent imaging, which is an emerging technique that can realize deep-tissue imaging with prolonged observation time.[1] Despite the advantages of two-photon microscopy, such as increased penetration depth (>500 μm), minimized fluorescence background, and less light scattering and tissue injury,[2] most previously reported two-photon probes were designed on the basis of single-emission intensity changes, which could be affected by instrumental efficiency, environmental conditions, and the concentration of probe molecules.[3−5] However, the advent of ratiometric probes eliminated most, if not all, such interferences by a built-in correction of the two emission bands. These probes subsequently proved to be more favorable for intracellular imaging compared with other fluorescent probes. Several strategies, including internal charge transfer, fluorescence resonance energy transfer (FRET), and through-bond energy transfer (TBET), have been adopted to design ratiometric probes. For ratiometric probes based on TBET, the donor is linked directly by an electronically conjugated bond with the acceptor, and energy transfer occurs through a conjugated bond without the need for spectral overlap, thus preventing donor and acceptor fragments from becoming planar.[6,7] As a result, such probes showed high energy transfer efficiency, two well-resolved emission peaks with high imaging resolution, less cross talk between channels because no spectral overlap between donor and acceptor is needed in TBET,[8] and dramatic amenability to molecular design. Again, however, previous TBET-based probes were still designed as single-photon probes with a rather short excitation wavelength, making it difficult to image tissue. To the best of our knowledge, no energy transfer-based ratiometric two-photon fluorescent probes suitable for tissue imaging have been previously reported.

The two-photon fluorescent activity of naphthalene derivatives was first reported by Cho et al.[9] (Figure 1). Based on their research, our group previously proposed a naphthalene derivative-based two-photon fluorescent probe, termed NHS1, which had a large two-photon active absorption cross-section (>120 GM) and could be used for rapid detection of H_2S, both in vivo and in vitro.[10] In order to acquire a better bioimaging result, we decided to combine the advantages of two-photon fluorescent imaging with TBET to develop a TBET-based ratiometric two-photon fluorescent probe. As a proof-of-principle, naphthalene derivative **a** was chosen as the TBET donor for its outstanding two-photon properties, while rhodamine spirolactam **b** was selected as the acceptor for its target-triggered "turn-on" fluorescent signal that can be easily distinguished, even by the naked eye (Figure 1). Moreover, TBET does not require spectral overlap between donor and

Received: April 22, 2014
Published: June 26, 2014

   dx.doi.org/10.1021/ja504015t | J. Am. Chem. Soc. 2014, 136, 9838−9841

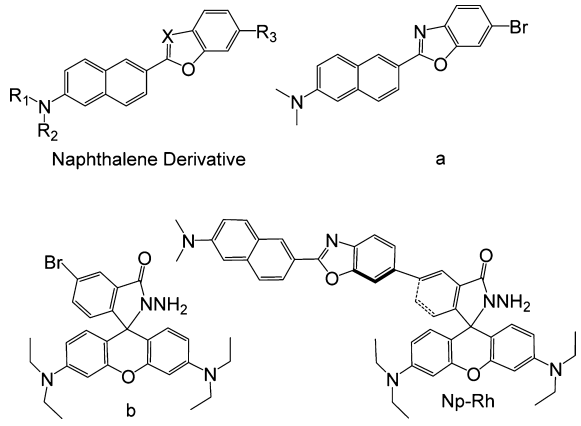

Figure 1. Structures of naphthalene derivatives, donor **a**, acceptor **b**, and two-photon TBET probe **Np-Rh**.

acceptor (see Figure S1) and can afford a large wavelength difference between the two emissions with less cross talk between channels[8] as well as higher energy transfer efficiency compared to classical FRET systems. To demonstrate the feasibility of this probe design, Cu^{2+} was chosen as the model target for its essential roles in the human body.[2,6a] This type of TBET-based ratiometric two-photon fluorescent probe, which we termed **Np-Rh**, exhibits a characteristic inertness toward pH changes from 2.0 to 10.0 and a large spectral shift between the two emissions (100 nm, from 475 to 575 nm), allowing for the high-resolution and sensitive ratiometric detection of targets. **Np-Rh** was then applied for ratiometric imaging in live cells and intact tissues with a thickness over 180 μm, and both achieved satisfactory results.

Np-Rh was synthesized via the Negishi cross-coupling reaction between the boronic acid pinacol ester of **a** and **b** with a yield of 85% (see Scheme S1 for synthetic route). All the reaction products were fully characterized by ^{1}H NMR, ^{13}C NMR, and mass spectrometry (see Supporting Information).

Density functional theory (DFT) calculations for the probe were first carried out by employing the B3LYP exchange functional and 6-31G* basis sets. The results are shown in Figure 2. When the spirocyclization is closed with rhodamine's conjugated structure being broken (for structures, see Figure S9), it was found that **Np-Rh** possesses a large energy gap (2.50 eV), such that the dihedral angle between the donor and acceptor is 30.74°. However, when it is opened with its conjugated structure being recovered, the gap is 2.57 eV, and the dihedral is 32.81°, demonstrating that the donor and the acceptor fragments are not coplanar, which is favorable for TBET.

The absorption property of **Np-Rh** (5 μM) was studied in buffered (Tris-HCl, pH = 7.4) water/C_2H_5OH (9/1, v/v) solution. In the absence of Cu^{2+}, only one absorption band at 395 nm was observed as a result of donor residue. When Cu^{2+} (0−50 equiv) was added, a new absorption band appeared at 525 nm, which belonged to the acceptor (rhodamine **b** residue). The solution's color changed from light-yellow to purple-red, allowing colorimetric detection of Cu^{2+} by the naked eye (Figure S2).

The changes in the **Np-Rh** fluorescence spectra upon the gradual addition of Cu^{2+} were further investigated (Figure 3). In the absence of Cu^{2+}, the acceptor exists in a closed-ring, colorless, nonfluorescent lactone form, and no energy transfer was observed from donor to acceptor. As a result, only the

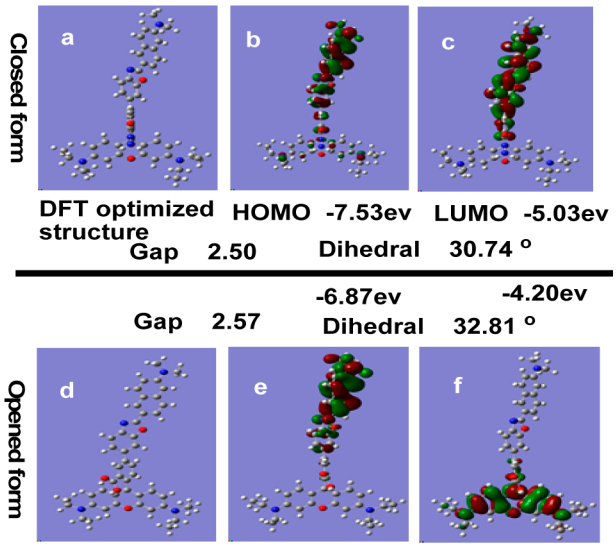

Figure 2. Density functional optimized geometries of the closed and opened forms of **Np-Rh**. (a, d) DFT-optimized structure of **Np-Rh** with the closed and opened forms. (In the ball-and-stick representation, carbon, nitrogen, and oxygen atoms are colored in gray, blue, and red, respectively. H atoms are omitted for clarity.) Molecular orbital plots (b, e) HOMO; (c, f) LUMO; and HOMO/LUMO energy gaps and dihedral of **Np-Rh** dyes in the closed or opened form.

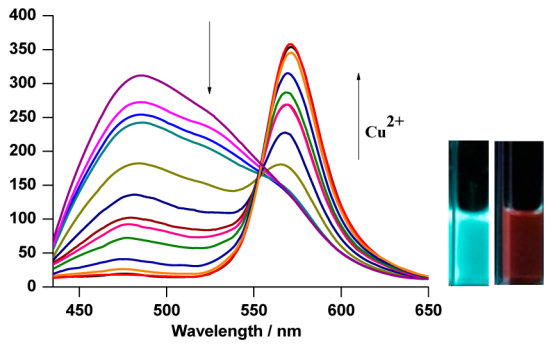

Figure 3. One-photon-excited fluorescent changes of **Np-Rh** (5 μM) in response to different concentrations of Cu^{2+} (0−50 equiv) in Tris-HCl/CH_3CH_2OH (9:1, v/v, 10 mM), pH = 7.4. λ_{Ex} = 420 nm. The inset picture shows fluorescence before and after the addition of Cu^{2+}.

green fluorescence of donor **a** was observed. However, adding Cu^{2+} generated an open-ring, colored, and fluorescent rhodamine **b** residue (acceptor), and the probe showed a strong fluorescence in the emission region of rhodamine **B**. As the addition of Cu^{2+} increased, the donor's characteristic emission peak (475 nm) gradually disappeared, while the characteristic emission peak (575 nm) of rhodamine **B** grew. In the present study, the detection limit (3σ/slope)[11] was estimated to be as low as 3.0×10^{-7} M (Figure S3) for Cu^{2+}, which is lower or comparable than those of previously reported fluorescent probes[12] and is sufficiently low for the detection of the submillimolar concentration range of Cu^{2+} found in many chemical and biological systems.[6a] At the same time, the energy transfer efficiency was calculated to be 93.7% (see SI and Figure S4). A previous report demonstrated that the TBET system was sometimes accompanied by FRET, resulting in the failure of energy transfer efficiency to reach 100%.[6a]

dx.doi.org/10.1021/ja504015t | J. Am. Chem. Soc. 2014, 136, 9838−9841

Selectivity experiments showed that only Cu^{2+} could trigger the receptor's open ring, while other ions in environmental and biological systems showed no perceptible effect, thereby demonstrating a high selectivity of the probe (Figures 4 and

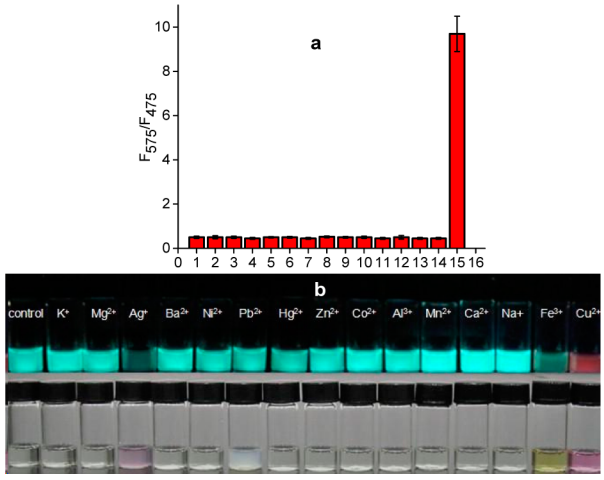

Figure 4. (a) Fluorescence ratio (F_{575}/F_{475}) of **Np-Rh** (5 μM) in the presence of various ions (50 μM) in CH_3CH_2OH/Tris-HCl (1/9, v/v, pH = 7.4, 10 mM), λ_{Ex} = 420 nm. The numbers from 1 to 15 correspond to K^+ to Cu^{2+}, respectively. (b) Fluorescence change (top) of **Np-Rh** (5 μM) in CH_3CH_2OH/Tris-HCl (1/9, v/v, pH = 7.4, 10 mM) with metal ions: control, K^+, Mg^{2+}, Ag^+, Ba^{2+}, Ni^{2+}, Pd^{2+}, Hg^{2+}, Zn^{2+}, Co^{2+}, Al^{3+}, Mn^{2+}, Ca^{2+}, Na^+, Fe^{3+}, and Cu^{2+} (50 equiv, from left to right) and change in color (bottom).

S5). We also studied the effect of pH on **Np-Rh** before and after addition of Cu^{2+}. The results showed that pH changes (from 2.0 to 10.0) had no obvious effect on the performance of our probe (Figure S6), indicating that the hydrolysis depended on copper ions, not pH value.

In order to study the two-photon properties of the probe, the two-photon active absorption cross-section of **Np-Rh** was calculated by using the following formula: $\delta = \delta r(S_s\ \Phi_r\ \phi_r\ c_r)/(S_r\ \Phi_s\ \phi_s\ c_s)$,[10] where the subscripts s and r denote the sample and reference molecule, respectively. In the absence of copper ions, the acceptor's ring is closed, and **Np-Rh** was calculated to have a two-photon active absorption cross-section of 115 GM (1 GM = 10^{-50} (cm ^{4} s)/photon) at 475 nm upon excitation at 780 nm (Figure 5a). In the presence of Cu^{2+}, the acceptor's ring is opened. Under laser excitation at 780 nm, the donor's fluorescent peak at 475 nm almost vanished, while a new strong fluorescent peak appeared at 575 nm (Figure 5b).

In order to evaluate the imaging performance of **Np-Rh**, we used this probe to detect Cu^{2+} in living biological samples, including cells and tissues. HeLa cells were chosen as the model cell line. After incubation with **Np-Rh** (5 μM) at 37 °C for 30 min, followed by laser excitation at 780 nm, the cells showed both single-photon and two-photon excited intense fluorescence in the cyan channel and weak fluorescence in the red channel, corresponding to strong fluorescence at 475 nm and weak fluorescence at 575 nm. After treating **Np-Rh**-cultured cells with 30 μM Cu^{2+}, the fluorescent signal intensity decreased in the cyan channel and increased in the red channel, corresponding to weak fluorescence at 475 nm and strong fluorescence at 575 nm (see results in Figure 6). The cytotoxicity experiment showed that the Np-Rh probe was nearly nontoxic to live cells with its concentration less than 14.0 μM (Figure S7). All above results and data showed that **Np-Rh**

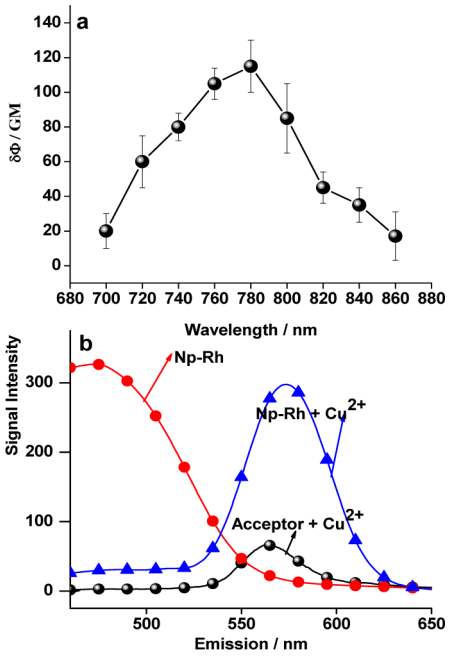

Figure 5. (a) Two-photon absorption cross-section of **Np-Rh** without adding Cu^{2+}. Rhodamine b was used as reference.[13,14] (b) Emission spectra of **Np-Rh** (5 μM, red line); **Np-Rh** (5 μM) in the presence of Cu^{2+} (50 μM, blue line) and acceptor **b** (5 μM) in the presence of Cu^{2+} (50 μM, black line). Two-photon excitation at 780 nm in Tris-HCl/CH_3CH_2OH (9/1, v/v), pH = 7.4.

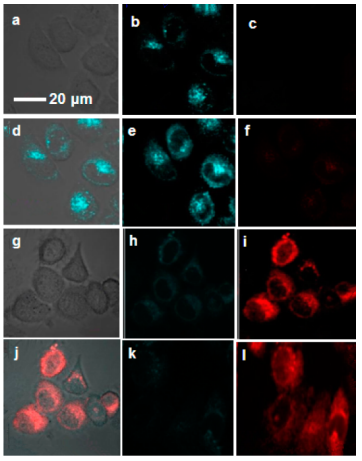

Figure 6. Images of HeLa cells treated with **Np-Rh**: (a) bright-field image of HeLa cells incubated with **Np-Rh** (5 μM); (b) fluorescent image of (a) from cyan channel; (c) fluorescence image of (a) from red channel; (d) overlay image of (a–c); (e) two-photon fluorescent imaging from cyan channel; (f) two-photon fluorescent imaging from red channel; (g) bright-field image of HeLa cells treated with **Np-Rh** (5 μM) for 30 min and then incubated with Cu^{2+} (50 μM) at 37 °C for 30 min; (h) fluorescent image of (g) from cyan channel; (i) fluorescent image of (g) from red channel; (j) overlay image of (g–i); (k) two-photon fluorescent imaging of cyan channel; (l) two-photon fluorescent imaging from red channel. One photon: λ_{Ex} = 405 nm; two Photon: λ_{Ex} = 780 nm. Cyan channel λ_{Em}: 450–530 nm and red channel λ_{Em}: 540–650 nm. Scale bar: 20 μm.

was cell membrane-penetrable and could be used for both single-photon and two-photon-excited live cell imaging.

We further used **Np-Rh** for tissue imaging of rat liver frozen slices, with **Np** (compound a) as a control. The changes of

dx.doi.org/10.1021/ja504015t | J. Am. Chem. Soc. 2014, 136, 9838–9841

fluorescence signal intensity with scan depth were determined by confocal multiphoton microscopy (Olympus, FV1000) in the *z*-scan mode. In the absence of Cu^{2+}, **Np** and **Np-Rh** were capable of tissue imaging at depths of 70−180 μm by TPM (Figure S8), indicating that **Np** and **Np-Rh** exhibit similar tissue penetration capability. When Cu^{2+} was added, depth scanning demonstrated that the corresponding **Np-Rh** product was capable of tissue imaging at depths of 50−180 μm by TPM, with tissue imaging results presented in two emission channels with different colors (see Figures 7 and S8). These data showed

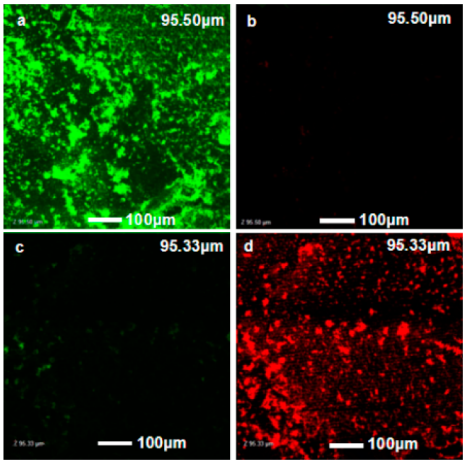

Figure 7. Two-photon imaging of a rat liver frozen slice stained with 10 μM **Np-Rh** at ~95 μm for 60 min (a, b), followed by treatment with 100 μM Cu^{2+} and incubated for another 60 min (c, d). The images were collected at 450−530 nm (green channel, a, c) and 540−650 nm (red channel, b, d) upon excitation at 780 nm with femtosecond pulses. Scale bars: 100 μm.

that **Np-Rh** has good tissue penetration and staining ability as well as ratiometric two-color (green and red) imaging performance with less cross talk between channels.

In summary, we have, for the first time, developed a novel small organic molecular two-photon ratiometric fluorescent probe, termed **Np-Rh**, which is based on TBET. This type of probe has such outstanding properties as dramatic resistance to pH changes, highly efficient energy transfer, rapid response time, and high selectivity. Moreover, since the two-photon probe has a long excitation wavelength (NIR), it can greatly reduce tissue injury and increase penetration depth, thus improving imaging results. Our experiment demonstrated that **Np-Rh** could be used as a robust two-photon TBET platform for constructing a two-photon fluorescent ratiometric sensor. We believe it will provide an effective tool for studying significant biological processes at the molecular level.

■ ASSOCIATED CONTENT

Ⓢ Supporting Information

Procedures and additional data. This material is available free of charge via the Internet at http://pubs.acs.org.

■ AUTHOR INFORMATION

Corresponding Author

tan@chem.ufl.edu

Notes

The authors declare no competing financial interest.

■ ACKNOWLEDGMENTS

This work was supported by the National Key Scientific Program of China (2011CB911000), NSFC (Grants 21325520, 21327009, J1210040, 21177036), the Foundation for Innovative Research Groups of NSFC (Grant 21221003), the National Key Natural Science Foundation of China (21135001), the National Instrumentation Program (2011YQ030124), the Ministry of Education of China (20100161110011), and the Hunan Provincial Natural Science Foundation (Grant 11JJ1002).

■ REFERENCES

(1) (a) Kim, H. M.; Cho, B. R. *Chem. - Asian J.* **2011**, *6*, 58. (b) Kim, H. M.; Cho, B. R. *Acc. Chem. Res.* **2009**, *42*, 863.
(2) Zhu, A. W.; Ding, C. Q.; Tian, Y. *Sci. Rep.* **2013**, *3*, 2933.
(3) Xu, Z. C.; Baek, K. H.; Kim, H. N.; Cui, J. N.; Qian, X. H.; Spring, D. R.; Shin, I. J.; Yoon, J. Y. *J. Am. Chem. Soc.* **2010**, *132*, 601.
(4) Han, Z. X.; Zhang, X. B.; Li, Z.; Gong, Y. J.; Wu, X. Y.; Jin, Z.; He, C. M.; Jian, L. X.; Zhang, J.; Shen, G. L.; Yu, R. Q. *Anal. Chem.* **2010**, *82*, 3108.
(5) (a) Zhao, Y.; Zhang, X. B.; Han, Z. X.; Qiao, L.; Li, C. Y.; Jian, L. X.; Shen, G. L.; Yu, R. Q. *Anal. Chem.* **2009**, *81*, 7022. (b) Li, C. Y.; Zhang, X. B.; Qiao, L.; Zhao, Y.; He, C. M.; Huan, S. Y.; Lu, L. M.; Jian, L. X.; Shen, G. L.; Yu, R. Q. *Anal. Chem.* **2009**, *81*, 9993.
(6) (a) Fan, J. L.; Zhan, P.; Hu, M. M.; Sun, W.; Tang, J. Z.; Wang, J. Y.; Sun, S. G.; Song, F. L.; Peng, X. J. *Org. Lett.* **2013**, *15*, 492. (b) Lin, W. Y.; Yuan, L.; Cao, Z. M.; Feng, Y. M.; Song, J. Z. *Angew. Chem., Int. Ed.* **2010**, *49*, 375. (c) Roopa, V. B.; Kumar, M.; Sharma, P. R.; Kaur, T. *Inorg. Chem.* **2012**, *51*, 2150. (d) Kumar, M.; Kumar, N.; Bhalla, V.; Singh, H.; Sharma, P. R.; Kaur, T. *Org. Lett.* **2011**, *13*, 1422.
(7) Wan, C. W.; Burghart, A.; Chen, J.; Bergström, F.; Johansson, L. B. A.; Wolford, M. F.; Kim, T. G.; Topp, M. R.; Hochstrasser, R. M.; Burgess, K. *Chem.—Eur. J.* **2003**, *9*, 4430.
(8) (a) Peleg, A.; Chung, Y. J. *Phys. Rev. A* **2012**, *85*, 1050. (b) Jin, M.; Berrout, J.; Chen, L.; O' Neil, R. G. *Cell Calcium* **2012**, *51*, 131. (c) Pang, J. J.; Gao, F.; Wu, S. M. *Vision Res.* **2007**, *47*, 384.
(9) (a) Kim, H. J.; Heo, Ch. H.; Kim, H. M. *J. Am. Chem. Soc.* **2013**, *135*, 17969. (b) Lim, C. S.; Masanta, G. T.; Kim, H. J.; Han, J. H.; Kim, H. M.; Cho, B. R. *J. Am. Chem. Soc.* **2011**, *133*, 11132. (c) Kim, H. M.; Jeong, B. H.; Hyon, J. Y.; An, M. J.; Seo, M. S.; Hong, J. H.; Lee, K. J.; Kim, C. H.; Joo, T.; Hong, S. C.; Cho, B. R. *J. Am. Chem. Soc.* **2008**, *130*, 4246. (d) Lee, J. H.; Lim, C. S.; Tian, Y. Sh.; Han, J. H.; Cho, B. R. *J. Am. Chem. Soc.* **2010**, *132*, 1216. (e) Bae, S. K.; Heo, C. H.; Choi, D. J.; Sen, D.; Joe, E. H.; Cho, B. R.; Kim, H. M. *J. Am. Chem. Soc.* **2013**, *135*, 9915.
(10) Mao, G. J.; Wei, T. T.; Wang, X. X.; Huan, S. Y.; Lu, D. Q.; Zhang, J.; Zhang, X. B.; Tan, W. H.; Shen, G. L.; Yu, R. Q. *Anal. Chem.* **2013**, *85*, 7875.
(11) Zhu, B. C.; Gao, C. C.; Zhao, Y. Z.; Liu, C. Y.; Li, Y. M.; Wei, Q.; Ma, Z. M.; Du, B.; Zhang, X. L. *Chem. Commun.* **2011**, *47*, 8656.
(12) (a) Jo, J. Y.; Lee, H. Y.; Liu, W. J.; Olasz, A.; Chen, C. H.; Lee, D. *J. Am. Chem. Soc.* **2012**, *134*, 16000. (b) Jung, H. S.; Kwon, P. S.; Lee, J. W.; Kim, J. I.; Hong, C. S.; Kim, J. W.; Yan, S. H.; Lee, J. Y.; Lee, J. H.; Joo, T.; Kim, J. S. *J. Am. Chem. Soc.* **2009**, *131*, 2009.
(13) Xu, C.; Webb, W. W. *J. Opt. Soc. Am. B* **1996**, *13*, 481.
(14) Albota, M. A.; Xu, Ch.; Webb, W. W. *Appl. Opt.* **1998**, *37*, 7352.